

Ultra-High-Beta Spherical Tokamak with Absolute Minimum-B in TS-3 Spherical Torus Experiments

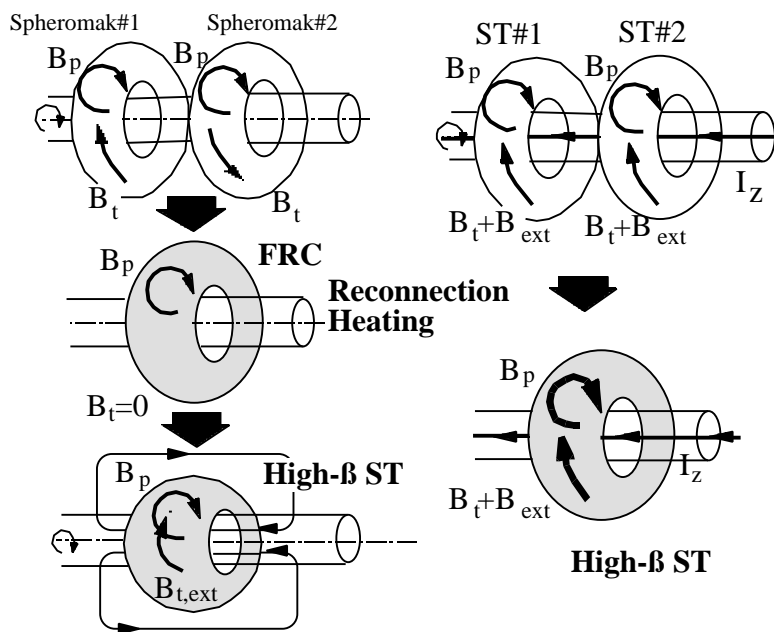
Y. Ono, M. Inomoto, Y. Ueda, M. Katsurai, T. Matsuyama, Y. Murata, T. Tawara

High Temperature Plasma Center, University of Tokyo,
7-3-1 Hongo, Bunkyo-ku, Tokyo 113-8656, Japan,
e-mail contact of main author: ono@katsurai.t.u-tokyo.ac.jp

Abstract. An absolute minimum-B configuration was obtained when applied external toroidal magnetic field transformed a field-reversed configuration (FRC) into an ultra-high-beta ($>50\%$) spherical tokamak (ST). High-power heating ($\sim 5\text{-}30\text{MW}$) of magnetic reconnection was used to form the oblate FRC and to increase thermal pressure (beta) of STs. High-beta STs with a variety of pressure and q profiles revealed their stability boundaries and possible ballooning collapses. The high-beta ST with maximum pressure gradient p' in the periphery was maintained stably, while another high-beta ST with maximum p' in the core collapsed due to high- n ($n > 8$) localized modes.

1. Introduction

The spherical tokamak (ST) has been investigated as an attractive extension of tokamaks, field-reversed configurations (FRCs) and spheromaks. It is expected to combine the long confinement time of tokamaks with the high-beta properties / compact reactor designs of FRCs and spheromaks. Peng and Strickler pointed out its compact and economical reactor concept[1] together with its high-beta property assured by the Troyon scaling[2]. Those advanced theoretical studies were followed by a number of world-wide ST experiments initiated from the Hiderberg ST experiment[3]. The START experiment with Neutral Beam Injection (NBI) achieved the averaged beta value as high as 20%, maintaining reasonably good confinement time up



(a) Transformation of FRC (b) ST Merging

FIG. 1. Two formation methods of high-beta STs by use of merging/magnetic reconnection.

those advanced theoretical studies were followed by a number of world-wide ST experiments initiated from the Hiderberg ST experiment[3]. The START experiment with Neutral Beam Injection (NBI) achieved the averaged beta value as high as 20%, maintaining reasonably good confinement time up

to 4ms[4]. The H-mode was also observed successfully in the START, revealing a confinement property of ST as good as tokamaks[5]. Those epoch-making results triggered the second-step Mega-Ampere(MA)-class ST experiments: NSTX[6] at the Princeton Plasma Physics Laboratory and MAST[7] at the Calham Laboratory.

Recent numerical analyses[8] suggested a possibility of ballooning-stable STs in ultra-high-beta regime, so-called second-stability. The second-stable ST has received increased attention because it will realize a real compact and high-beta reactor which can be extended to a D-D reactor in future. Unlike the conventional tokamaks[9], the ST with strong toroidal effect[8] has a narrow window connecting the first and second stability regimes in the dq/d (magnetic shear) - dp/d (pressure gradient) diagram for high-n ballooning instabilities, where q is the safety factor, p is the plasma thermal pressure and ψ is the poloidal flux function. This fact indicates a possibility of ultra-high-beta ST formation in the second stability regime.

A new formation of ultra-high-beta spherical tokamak has been developed in the TS-3 spherical torus device using an oblate FRC[10]. As shown in Fig. 1(a), two spheromaks with opposing toroidal field B_t were merged axially to produce an oblate FRC[11,12]. Their magnetic reconnections converted the whole toroidal magnetic energy of the merging spheromaks into ion thermal energy of the produced FRC through ion acceleration effect of reconnected field lines. Then, applied external B_t transformed it into an ultra-high-beta ST. This method eliminates a difficulty of forming a hollow current profile by fast ramp-up of ohmic heating (OH) coil current and possibly provides us a new direct path to the second stable ST, as shown in Fig. 2. We produced another high-beta ST using two merging low-beta STs as shown in Fig. 1(b). The ion heating effect of magnetic reconnection converted a part of poloidal magnetic energy of the low-beta STs into ion thermal energy of the high-beta ST.

An important question then arises as to by what mechanism the high-beta STs are produced / maintained and what instability affects their stability. We measured directly for the first time detailed profiles of ion and electron temperatures, electron density and q -value to plot the s - q diagram of the STs and found its relation to high-n mode activity and disruption. This paper addresses three important issues of the ultra-high-beta ST equilibria and stabilities:

- (1) absolute minimum-B characteristics of the ultra-high-beta STs,
- (2) confirmation of their second stable equilibria and
- (3) collapses of the ultra-high-beta STs due to high-n mode activities.

Formations of STs with various pressure and q profiles revealed their high-beta property and stability boundary.

2. Experimental Setup

The TS-3 merging device[10] was used to study the ultra-high-beta regime of STs with aspect ratio $A \approx 1.5$. As shown in Fig.3, its cylindrical vacuum vessel with length of 1m and diameter of 0.8m has two poloidal (PF) coils for poloidal flux injection and two sets of eight electrode pairs for toroidal flux injection. They can produce the two spheromaks whose toroidal field B_t polarities are determined by those of the electrode discharge currents. As shown in Figs. 1(a) and (b), this experiment used two types of mergings to produce high-beta

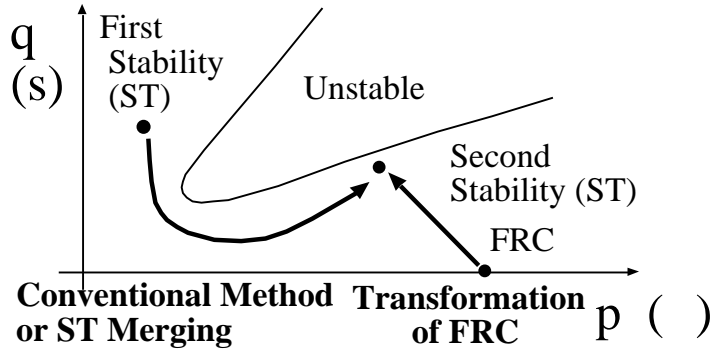


FIG. 2. Magnetic shear q_{ψ} - pressure gradient p_{ψ} diagram of ST and three possible formation methods of second-stable ST.

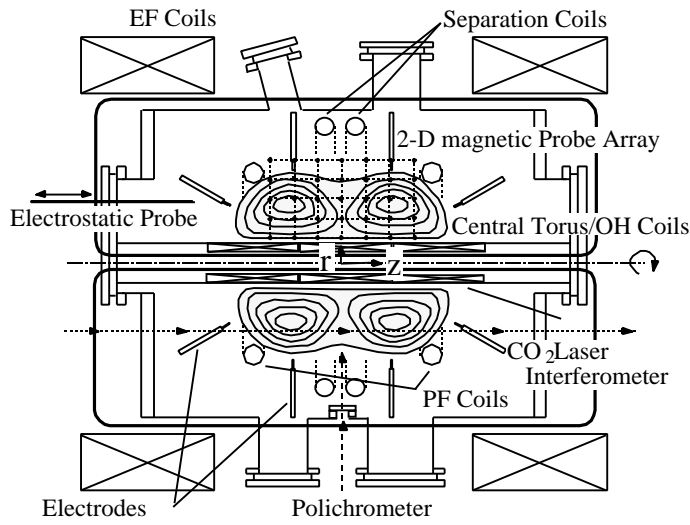


FIG. 3. TS-3 ST/CT Merging Device ($R=0.18-0.22m$, $R/a=1.5$, $B_0 < 2kG$, $T_i=10-200eV$, $T_e=10-40eV$, $n_e=2-10 \times 10^{19}m^{-3}$).

200 μ sec. A 2-D array of magnetic probe composed of 200 pickup coils was inserted on the r-z plane of the vessel to measure directly the 2-D magnetic field profile. A polychrometer with optical multi-channel analyzer was used to measure radial ion temperature T_i profiles by means of the Doppler widths of carbon and hydrogen lines. An electrostatic probe array was inserted to measure their radial profiles of electron temperatures T_e and densities n_e . Poloidal flux contours, current density profiles and plasma pressure profiles were calculated using this 2-D magnetic field profiles and T_i , T_e , and n_e profile measurements.

3. Experimental Results

Figure 4 shows the time evolution of poloidal flux contour with toroidal field amplitude (red and blue colors) during the ultra-high-beta ST formation. From $t=40\mu$ sec to 50μ sec, two merging spheromaks with opposing B_t were transformed into an FRC without B_t . Figure 5 shows time evolutions of plasma current I_p , electron density n_e , ion and electron temperatures

STs with a variety of pressure and q profiles. In Fig. 1(a), two spheromaks with opposing B_t were merged together to produce an FRC. Then, external toroidal field up to 1kG was applied to the produced FRC with rise time of 15 μ sec using a center toroidal coil, transforming it into an ultra-high-beta ST. In Fig. 1(b), two merging STs with the same B_t polarity were used to heat the ST through their magnetic reconnection[10]. The plasma heating powers of the former and latter methods were about 30MW and 5-10MW, respectively. Each merging toroid initially had major radius R 0.18-0.22m, aspect ratio A 1.5, T_i T_e 10eV, n_e $2-10 \times 10^{19}m^{-3}$ and $B < 2kG$. Their merging speed was controlled by magnetic pressure of the PF coil currents and separation coil currents on the midplane. An OH coil (diameter 0.12m) was used to provide volt-second for current sustainment of STs for 100-

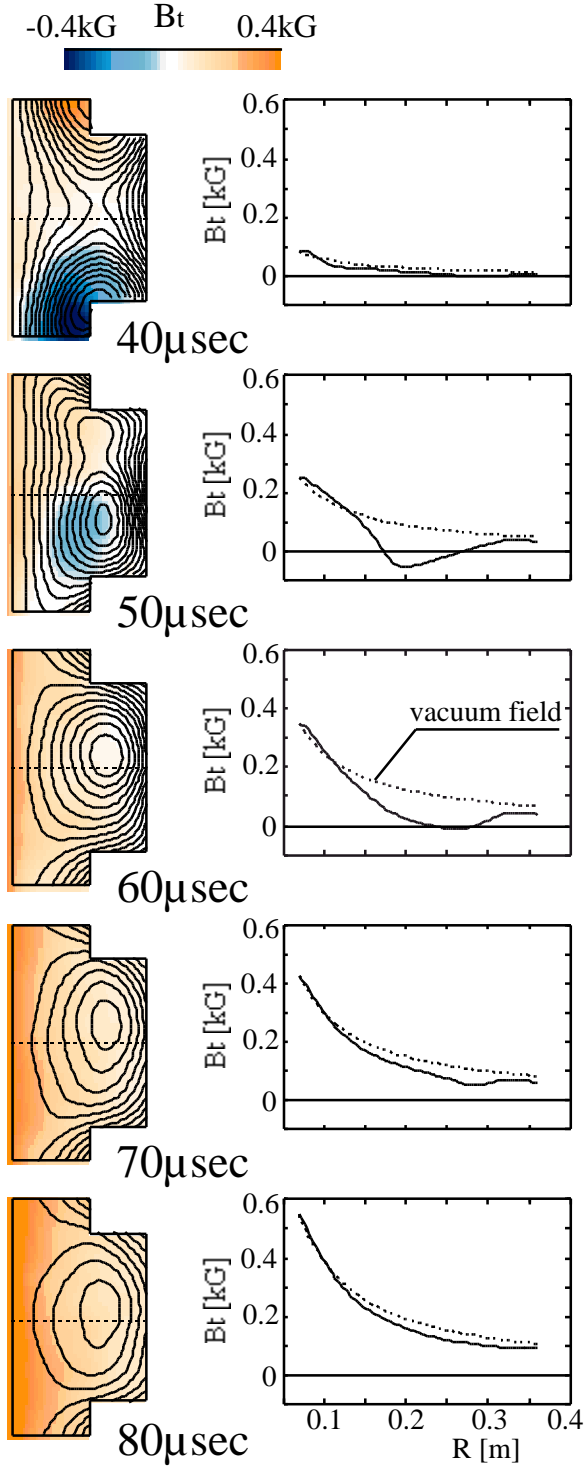


FIG. 4. Time evolutions of poloidal flux contour with B_t field amplitude and radial B_t profile during the ultra-high-beta ST formation.

B_t from $t=50\mu\text{sec}$ to $70\mu\text{sec}$. About 50-80% of the thermal energy was maintained during the equilibrium transition to the high-beta ST with β 0.4-0.7 and T_i 150eV ($\gg T_e$ 10-20eV),

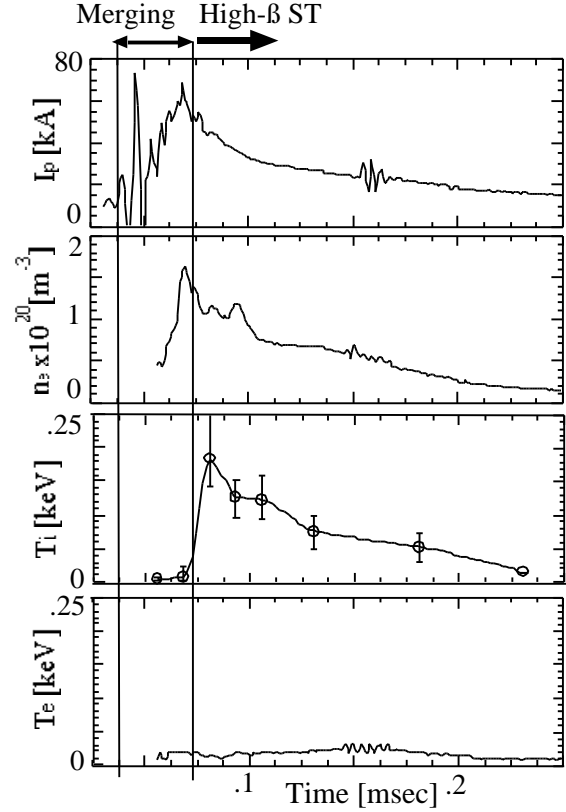


FIG. 5. Time evolutions of plasma current I_p , electron density n_e ($R=0.2\text{m}$), ion/electron temperatures T_i , T_e ($R=0.22\text{m}$ and 0.24m) during the ultra-high-beta ST formation.

T_i , T_e at $R=0.2-0.25\text{m}$ during the whole process. During the FRC formation, the volume averaged beta increased from 0.05-0.1 to 0.7 due to significant ion heating from 10eV to 200eV. The formation of FRC is attributed to the conversion effect of magnetic reconnection from magnetic energy of opposing B_t to ion thermal energy of the FRC[11]. Then, the external B_t was applied to the oblate FRC with rise time of $15\mu\text{sec}$ right after its formation. During this process, volt-second of the OH coil sustained the plasma current for 100-200 μsec . Figure 4 indicates that the FRC without B_t was transformed stably into a new ST with finite

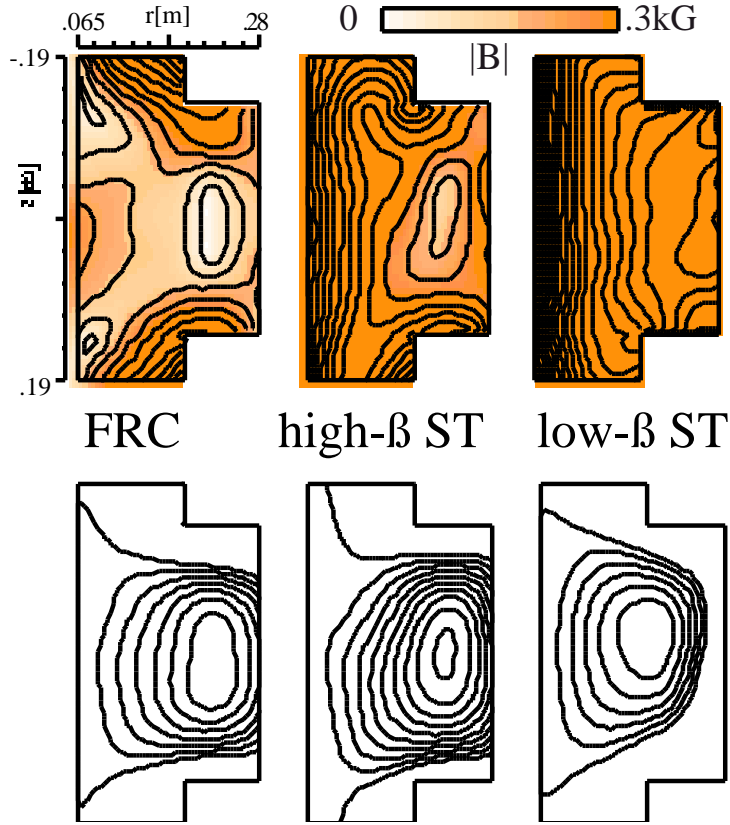


FIG. 6. $|B|$ and poloidal flux contours of the FRC, the ultra-high-beta ST and the low-beta ST.

based on detailed measurements of T_i , T_e and n_e . Figure 4 also shows the radial B_t profiles of the ultra-high-beta ST. Note that the B_t profile (solid line) of the ultra-high beta ST was located in the diamagnetic side of the vacuum B_t profile (dotted line) in sharp contrast with the peaked B_t profiles of the conventional low-beta STs[10]. The poloidal beta of the ultra-high beta ST was estimated as high as 1-1.2. After the B_t application, the ion temperature and the plasma current were observed to decrease slowly because no additional heating method except the low-power OH coil heating was used after the initial high power heating (30MW) of the merging. Our new formation method was found to fully suppress the strong para-

magnetic B_t , probably because of the new path to the high-beta ST shown in Fig. 2.

A question is by what mechanism the ultra-high beta ST was maintained stably in the possible second-stability regime. Recently, we found that the high-beta ST was equipped with a unique absolute minimum-B profile. Figure 6 shows the r - z contours of $|B|$ and poloidal flux of the initial FRC, the produced ultra-high-beta ST and the low-beta ST. The low-beta ST was produced by the conventional z -theta pinch method (no merging) under constant external B_t . The ultra-high-beta ST with diamagnetic B_t was observed to have an absolute minimum-B profile in sharp contrast with the low-beta ST without $|B|$ -minimum. The external B_t helps the ultra-high-beta ST to have a minimum-B profile more widely than the FRC with minimum-B region locally around the magnetic axis. This absolute minimum-B profile was maintained for 50-80 μ sec but slowly disappeared because of the low-power additional heating of OH coil after the merging. The above mentioned fact suggests that the absolute minimum-B can be a possible cause for the stable sustainment of the ultra-high-beta ST. The minimum-B area was maximized when the center toroidal coil current I_{tc} was set around an optimum value of 30kA. If I_{tc} was smaller than 30kA, a narrow low- $|B|$ area tends to be formed between the core region and the center-top / -bottom regions, decreasing the minimum- $|B|$ area significantly.

An important question is whether the observed high-beta ST is located in the second

stability regime or not. Figures 7(a), (b) and (c) show q ($=dq/d\psi$: magnetic shear)- p ($=dp/d\psi$: pressure gradient) diagrams (s - ψ diagram) of the initial FRC, the ultra-high-beta ST and the low-beta ST mentioned before. Both of p and q were calculated as functions of the poloidal fluxes ψ , based on the measured profiles of B , T_i , T_e and n_e . Since the low-beta ST had the peaked pressure p profile, its pressure gradient p was small in the periphery and relatively large in the core, as shown in Fig. 7(c). However, the ultra-high-beta ST with hollow p and q profiles was observed to have the largest p and q in the periphery and relatively small p and q in the core, as shown in Fig. 7(b). The high- n ballooning-mode is expected to appear above the dotted lines in Figs. 7. These results strongly suggest that the q - p profile of the low-beta ST is located in the first stability regime and that of the ultra-high-beta ST in the second stability regime. As shown in Fig. 7(a), the initial FRC also had the largest p in the periphery, indicating the close relationship between the FRC and the high-beta ST in the second stability regime. When external toroidal field was applied to the FRC, its peripheral region obtained the maximum q in addition to the maximum p , indicating the transformation of the FRC into the ultra-high-beta ST.

Recently, we artificially increased the magnetic shear q (or center toroidal coil current I_{tc}) or the pressure gradient p to confirm the expected ballooning unstable regime. Figure 7(d) shows the q - p diagram of the unstable high-beta ST whose I_{tc} was 33% larger than that of (b). The large I_{tc} tends to increase the magnetic shear of the ST, approaching its q - p profile to the possible ballooning unstable regime. Once its q - p profile entered the unstable regime, its thermal pressure was

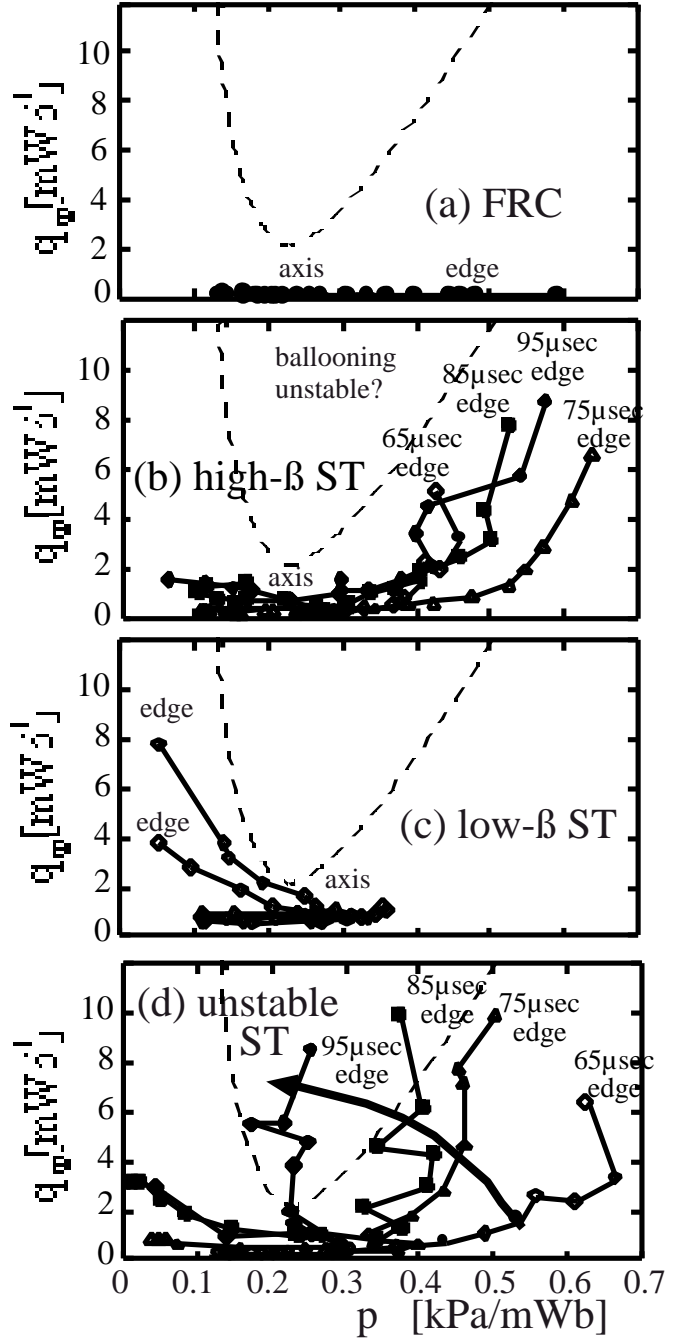


FIG. 7. q_{ψ} - p_{ψ} diagrams of the FRC (a), the ultra-high- β ST (b), the low- β ST (c) and the unstable high- β ST (d).

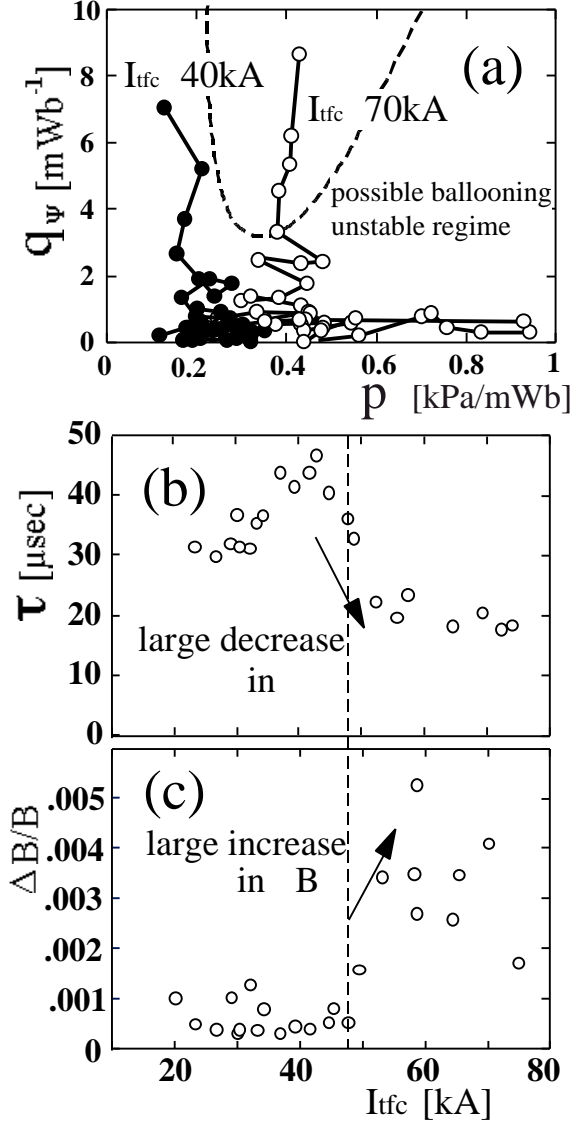


FIG. 8. (a) q_ψ - p_ψ diagrams of high- β STs with two different I_{tfc} , (b) $\Delta B/B$ around the separatrix and (c) decay time τ of high-beta ST as a function of I_{tfc} .

of 45-50kA. It is noted that the magnetic fluctuation was localized around the separatrix and that its toroidal mode number was larger than $n=8$. These facts indicate that profile control of high-beta ST is essential to its stable sustainment. They strongly suggest that the high-beta ST disrupted due to ballooning instability when its q - p diagram entered the unstable regime.

4. Discussions

The above mentioned results clearly indicate that the ultra-high beta ST was produced by use of an oblate FRC. Unlike the conventional low-beta ST with the peaked pressure profile, the ultra-high beta ST had the largest pressure gradient and magnetic shear in the periphery, indicating that it was located in the second stability regime. The ultra-high beta ST

observed to be annihilated within $20\mu\text{sec}$. This result agrees well with the following disruption of the high-beta ST observed around $t=90\mu\text{sec}$.

We also measured the high- n / high-beta instability when the low-beta ST was heated by the merging of two STs. As shown in Fig. 1(b), two ST merging generated significant heating power as large as 5-10MW for about 20-30 μsec . In this case, the high-power heating of ST merging was observed to move its q - p profile from left to right in Fig. 7(c), possibly touching the possible unstable regime. Figure 8(a) shows the q - p diagrams of thus formed high-beta STs with different I_{tfc} ($I_{\text{tfc}}=40\text{kA}$ and 70kA). As I_{tfc} was increased, the pressure gradient p was also observed to increase more markedly than magnetic shear q probably because the high toroidal field improved the thermal energy confinement significantly. Figures 8(b) and (c) show the magnetic fluctuation $\Delta B/B$ around the separatrix and decay time (poloidal flux / loop voltage, right after the merging) of the high-beta STs as a function of I_{tfc} . The high-beta ST collapsed abruptly and magnetic fluctuation $\Delta B/B$ also increased by factor 10 when I_{tfc} exceeded a threshold value

was found to have an absolute minimum-B configuration that provided a basic stability against the high-beta ballooning and interchange modes. In agreement with this fact, its equilibrium was maintained stably for 100-200 μ sec, which is limited by the capacitor bank energy. However, the plasma beta slowly decreased and the absolute minimum-B configuration slowly disappeared due to low additional heating power of OH coil. The present setup enabled us to study the high-beta properties of ST for about 50-100 μ sec. Probably, it is reasonable to conclude that the produced high-beta ST was stable against the ballooning mode and current-driven mode for about 30-50 Alfvén time in the present experimental condition. However, some high-power additional heating like Neutral Beam Injection (NBI) is needed to study the instabilities whose growth time are longer than 30-50 Alfvén time. Especially, it is worth studying its stability against current-driven modes caused by the hollow current profile essential to the high-beta ST. In future, the proposed formation method of ultra-high-beta ST is probably useful as an easy startup of the second stable ST or as a current drive together with NBI or additional multiple mergings to maintain the high heating power.

5. Summary and Conclusions

In summary, we made clear the high-beta(>70%) features of ST using a unique transformation of the oblate FRC into the high-beta ST. The ultra-high-beta ST was found to have an absolute minimum-B configuration, probably causing the stable sustainment of this ST for 100-200 μ sec. This high-beta ST had the largest magnetic shear and pressure gradient in the periphery, while the conventional low-beta ST had the largest pressure gradient in the core. The high-beta ST was maintained stably or collapsed depending on whether its $q - p$ profile was located in the stable regime or in the unstable regime for ballooning instability. The high- n magnetic fluctuation was found to be a main cause for the disruption of the high-beta ST in the ballooning unstable regime.

References

- [1] PENG, Y.-K. M., and STRICKLER, D. J., Nucl. Fusion **26**, 769, (1986).
- [2] TROYON, F. et al., Plasma Phys. Controlled Fusion **26**, 209, (1984).
- [3] BRUNS, H. et al., Nucl. Fusion **27**, 2178, (1987).
- [4] GRYAZNVICH, M. et al., Phy. Rev. Lett. **80**, 3972, (1998).
- [5] SYKES, A. et al., Phy. Rev. Lett. **84**, 495, (2000).
- [6] SPIZER, J. et al., Fusion Technol. **30**, 1337 (1996).
- [7] SYKES A., Phys. Plasmas **4**, 1665, (1997); HENDER, T. C. et al., ibid **6**, 1958, (1999).
- [8] MILLER, R. L. et al., Phys. Plasmas **4**, 1062, (1997).
- [9] WESSON, J., in "Tokamak", (Clarendon Press, Oxford 1987), p.160.
- [10] ONO, Y. and INOMOTO, M., Phys. Plasmas **7**, 1863, (2000).
- [11] ONO, Y. et al., Phys. Rev. Lett. **76**, 3328, (1996).
- [12] ONO, Y. et al., in Plasma Physics and Controlled Nuclear Fusion Research 1992, Wurzburg (International Atomic Energy Agency, Vienna, 1993) **2**, p.619.